Nat. Hazards Earth Syst. Sci., 11, 1003–1009, 2011
www.nat-hazards-earth-syst-sci.net/11/1003/2011/
doi:10.5194/nhess-11-1003-2011

Natural Hazards and Earth System Sciences

Characteristics of long-term regional seismicity before the 2008 Wen-Chuan, China, earthquake using pattern informatics and genetic algorithms

H.-C. Li and C.-C. Chen

Institute of Geophysics, National Central University, Jhongli, Taiwan

Received: 21 December 2010 – Accepted: 2 February 2011 – Published: 30 March 2011

Abstract. To understand the generation of the 2008 Wenchuan, China earthquake, we developed a strategy to objectively identify possible seismic precursors. Based on the pattern informatics (PI) method, the pattern of seismic anomaly was identified by the aid of genetic algorithms (GA) to be highly similar to the spatial distribution of the Wen-chuan earthquake sequence. We found that smaller earthquakes ($M < 4.4$) showed a linear relationship of Gutenberg-Richter (G-R) distribution. However, the frequency of the intermediate earthquakes ($M \geq 4.4$) showed an uplift. This uplift supports the seismic activation hypothesis developed by Rundle et al. (2000b) and is similar to the case of the 1999 Chi-chi, Taiwan earthquake sequence reported by Chen (2003).

1 Introduction

The Si-chuan basin in China was struck by a sudden and extremely destructive earthquake on 12 May 2008 06:28:04 (UTC). Since this region is located where the Himalaya mountain belt and the Eurasian plate collide, the Si-chuan basin is a high seismic area. According to the official report, about seventy thousand people were killed and three hundred and seventy four thousand people injured in this catastrophic event. However, in contrast to the serious damage caused by this big earthquake, no effective short-term warning was issued before the occurrence of the main shock. Although several researchers have pointed out the high seismic hazard in this region, no details have been provided about how such a big earthquake is generated (Densmore et al., 2007; Long et al., 2006). This situation motivated us to research the characteristics of the seismicity before the Wen-chuan earthquake using a developed statistical tool, pattern informatics.

Pattern informatics (PI) was developed to evaluate the anomaly of seismicity in a specific region during an interval of interest. The fundamental concept is built up from numerical simulations of driven threshold systems (Egolf, 2000; Ferguson et al., 1999; Klein et al., 2000; Rundle et al., 1995, 2000a) and the physical meaning is explained by phase dynamics. After dividing the research region by a planar box of regular size, seismic anomaly in a box during an interval is evaluated by comparing its past long-term average seismicity and seismicity in other boxes. In the PI method, both seismic activation and quiescence are considered and expressed numerically as seismic anomaly. In several scientific works, the spatial distributions of stronger seismic anomalies are similar to upcoming earthquakes, including big ones (Chen et al., 2006; Nanjo et al., 2006; Tiampo et al., 2006). These results imply that a seismic anomaly is a possible indicator of upcoming big earthquakes. However, important parameters involved in the PI method; for example: magnitude, depth and initial or termination time, are usually coupling in selecting seismic data. Coupling of parameters absolutely raises the difficulty in identifying seismic information from noisy and complex regional seismicity.

In this work, we are concerned with possible seismic anomalies before the Wen-chuan earthquake at first. Based on the assumption of PI method, upcoming earthquakes tend to occur in the area which the evaluated seismic anomaly is much stronger than a background average. Thus, we developed a strategy to objectively identify seismic anomaly whose spatial distribution could be similar to the Wen-chuan main shock and aftershocks. The seismic anomaly was caused by changes of seismicity during two successive intervals before the Wen-chuan earthquake. We have

Correspondence to: H.-C. Li
(93642005@cc.ncu.edu.tw)

suggested that, by researching the characteristics of seismicity during the intervals, important information about the generation of big earthquakes could be provided.

Regional seismicity is mainly recorded by the national and regional seismic networks. Both networks are maintained by China Earthquake Administration (CEA). The initial times of the national and regional catalogs are initiated from 1 January 1970 (UTC) and 1 January 2001 (UTC) respectively. For a longer time span of the seismic record, we applied the national catalog in this research.

In this research, the genetic algorithm (GA, Goldberg, 1989; Holland, 1975) was applied as the selection tool for parameters in the PI method. In GA, important PI parameters were taken as genes in each chromosome of an initial population. For each chromosome, a PI map was generated after applying a gene set in the PI method. The performance of a PI map depended on the similarity between the distribution of hotspots on a PI map and the distribution of the main shock and following aftershocks. A PI map performed better if two distributions were more similar. The relative operating characteristic (ROC) diagram (Jolliffe and Stevenson, 2003) was applied to quantitatively evaluate the performance of each PI map. Once the best solution was determined, we turned to respective statistical behavior and characteristics of seismicity during baseline and change intervals.

From the best solution we obtained, the baseline interval was from 1 October 1984 to 30 September 2001 and the change interval was from 1 October 2001 to 31 January 2008 (UTC). The seismicity during both intervals was displayed as curves in a Gutenberg-Richter (G-R) frequency-magnitude distribution to show respective characteristics. For the change interval, the G-R curve showed a linear pattern in smaller magnitude earthquakes. But, for intermediate magnitude earthquakes, the linear pattern broke and the G-R curve showed an uplift in frequency. This uplift conformed to the characteristics of seismic activation in the seismic activation hypothesis developed by Rundle et al. (2000b).

In this research, the combination of GA and PI showed high efficiency in objectively searching for the important seismic anomalies. The result showed that seismic activation began roughly six years before the Wen-chuan earthquake. A similar characteristic is reported for the Chi-chi earthquake by Chen, too (Chen, 2003). However, more case studies are still necessary for further information about generation process of big earthquakes.

2 Methods: Pattern informatics

Pattern informatics (PI) was first developed by Rundle et al. (2002) and Tiampo et al. (2002), and is applied by several researchers on different seismic active regions (Chen et al., 2005; Nanjo et al., 2006; Tiampo et al., 2006). The calculation algorithm we used was modified by Chen et al. (2005). Although the details of calculations are not the same for each version, the fundamental concepts are common. In many numerical simulations to non-equilibrium systems, measurements of the inherent physical quantity of each model display a statistical equilibrium property (Egolf, 2000; Ferguson et al., 1999; Klein et al., 2000; Rundle et al., 1995, 2000a). The ensemble summation of inherent physical quantity keeps nearly a constant and merely fluctuates to a lower extent. This statistical equilibrium property is observed in real fault networks, too (Tiampo et al., 2007). In PI, fluctuations of statistical quantity in a small fault segment are suggested to contain important information about the evolution of seismicity in a fault network. Thus PI is applied to research fluctuations of long-term earthquake numbers in real fault systems.

The details of the modified PI are addressed below. Earthquakes in a seismic catalog were selected according to predefined ranges of space, depth and magnitude. The spatial range of interest was first divided by regular boxes. In this research, the square planar box was used and the length of each side was 0.1°. The total number of square boxes was named N_b.

There were five temporal parameters in the modified PI method. The beginning of the catalog we used was defined as T_0. It was unnecessary to be the initial recording time of the catalog. A later temporal point after T_0 was T_1.

The interval between T_0 and T_1 was the "baseline interval". A later point after T_1 was T_2. The interval between T_1 and T_2 was the "change interval". The last temporal parameter after T_2 was T_3. The interval between T_2 and T_3 was the "forecasting interval". Earthquakes which occurred in the "forecasting interval" were selected by predefined magnitude threshold and were formed into a set of targets. A series of sequent temporal points between T_0 and T_1 was defined as T_b. The application of T_b provided different initial times in calculating seismic rates and rate changes in PI. For statistical stability, the last T_b was selected to satisfy a condition: the length of interval, T_b to T_1, was equal to change interval, T_1 to T_2. Total number of earthquakes in a box x_i during interval T_b to t was defined as $N(x_\mathrm{i}, T_\mathrm{b}, t)$. The average seismic rate was evaluated by following equation:

$$R(x_\mathrm{i}, T_\mathrm{b}, t) = \frac{N(x_\mathrm{i}, T_\mathrm{b}, t)}{t - T_\mathrm{b}} \tag{1}$$

The parameter t could be T_1 or T_2 to describe long-term average seismic rates during T_b to T_1 or T_b to T_1, respectively. To account for the change of seismicity during the "change interval", the seismic rate change was defined by Eq. (2).

$$\Delta R(x_\mathrm{i}, T_\mathrm{b}) = R(x_i, T_\mathrm{b}, T_2) - R(x_i, T_\mathrm{b}, T_1) \tag{2}$$

For a specific box x_i, the application of T_b enabled us to evaluate $R(x_i, T_\mathrm{b}, t)$ and $\Delta R(x_i, T_\mathrm{b})$ based on different initial times. It could prevent possible statistical bias when T_0 was used as the only initial time. Thus, for each box x_i, there was a series of seismic rates and seismic rate changes due to a series of T_b. Considering a specific box, T_b normalization

was applied to a series of seismic rate changes in the box to give each T_b a statistical relative evaluation:

$$\Delta R_t(x_i, T_b) = \frac{\Delta R(x_i, T_b) - \overline{\Delta R}(x_i)}{\sigma(\Delta R\ (x_i, T_b))} \quad (3)$$

In Eq. (3), $\overline{\Delta R(x_i)}$ was the average and $\sigma(\Delta R(x_i, T_b))$ was the standard deviation over all T_b of box x_i.

After T_b normalization, a specific T_b was considered now. To statistically evaluate the seismic rate change of box x_i, a spatial normalization was applied for comparing to seismic rate changes of other boxes:

$$\Delta R_{xt}(x_i, T_b) = \frac{\Delta R_t(x_i, T_b) - \overline{\Delta R_t}(T_b)}{\sigma(\Delta R_t(x_i, T_b))} \quad (4)$$

Similar to Eq. (3), $\overline{\Delta R_t}(T_b)$ was the spatial average and $\sigma(\Delta R_t(x_i, T_b))$ was the spatial standard deviation over all boxes for a specific T_b.

After spatial normalization, an average rate change of box x_i was evaluated by averaging $\Delta R_t(x_i, T_b)$ over all T_b:

$$\overline{\Delta R_{xt}(x_i)} = \frac{1}{N(T_b)} \sum_{T_b} \Delta R_{xt}(x_i, T_b) \quad (5)$$

To evaluate seismic activation and seismic quiescence simultaneously, we applied squares of average rate changes. The background value was defined as the spatial average of squared seismic rate changes over all boxes. To further emphasize larger changes beyond the spatial average, the background average was subtracted from all squared rate changes to get the relative amplitude for each box:

$$P(x_i) = \overline{(\Delta R_{xt}(x_i))^2} - \frac{1}{N(x_i)} \sum_{x_i} \overline{(\Delta R_{xt}(x_i))^2} \quad (6)$$

In our application, spatial boxes which relative amplitude exceeded a predefined threshold were selected as hotspots. The hotspots were actually used to evaluate the performance of a PI result.

There were two major differences between the modified PI method addressed above and the original version. The first one was statistical quantity used for seismic rate change. In the original PI, average seismic rates in Eq. (1) were spatially normalized, then used in Eq. (2) for seismic rate change. Another major difference was the application of T_b normalization in the modified PI. For a box which had high seismicity persistently, large fluctuations of seismic rate were essentially easier to be determined due to numerous, episodically occurred earthquakes in it. The application of T_b normalization could eliminate some kind of fluctuations similar to background noise and highlight stronger rate changes.

The relative intensity (RI) was developed as a comparison with relative probability. It was defined as the logarithmic ratio of past seismicity during the baseline interval by following equation:

$$\mathrm{RI}(x_i) = \log_{10}\left(\frac{N(x_i, T_0, T_1)}{\max(N(x_1, T_0, T_1))}\right) \quad (7)$$

The maximum of earthquake number among all the boxes was used as a normalization factor. Thus the maximum of RI was 0 and all other values were negative.

A proper statistical tool is always necessary to evaluate statistical results adequately. We applied the relative operating characteristic (ROC) diagram, a binary evaluation method, in this research (Jolliffe and Stevenson, 2003). It can evaluate success and failure rates at the same time.

The distribution of a predefined set of earthquakes was a target to match. We applied a looser standard to define a successful match. For each hotspot which was located in a specific box, eight nearest boxes around the hotspot were taken as its expansion.

To each box, there were four possible situations. First, the box could be a selected hotspot, and there was at least one target earthquake in its neighborhood expansion. Second, the box could be a selected hotspot, but there was no target earthquake in its expansion. Third, the box was not a hotspot, but there was at least one target earthquake in it. Four, there was neither a hotspot nor a target earthquake in a box. The total number of each kind of boxes was named a, b, c and d in turn. The total number of all boxes was named N, and thus was equal to (a + b + c + d). In the ROC diagram, the y-axis was defined as "Hit rate" and the y-value was calculated by a/(a + c). The x-axis was "False rate" and the x-value was calculated by b/(b + d). The maximums of both axes were 1.

The performance of a PI result was evaluated by the similarity between the hotspots and the target earthquakes in spatial distribution. A series of hotspot thresholds were applied in descending order. The spatial coverage of the hotspots would increase with descending hotspot thresholds. The values of the four parameters and corresponding "Hit rate" and "False rate" were changed, too. Thus the performances of the PI and RI maps was evaluated by the area confined by the ROC curve and two axes. The best forecast is the one having the largest area. Areas for a perfect forecast, a random guess and a completely failed forecast were 1, 0.5 and 0 in turn. This area evaluation by the ROC diagram was used in the genetic algorithm. The details of the genetic algorithm are addressed in the next section.

3 Method: Genetic algorithms

Genetic algorithms (GA) are widely applied for optimization of problems in many fields. The fundamental element in (GA) is the gene. Important parameters of a problem in research are encoded to corresponding genes. Several genes compose a genetic string, called a chromosome or an individual. Each chromosome has an associated fitness measure

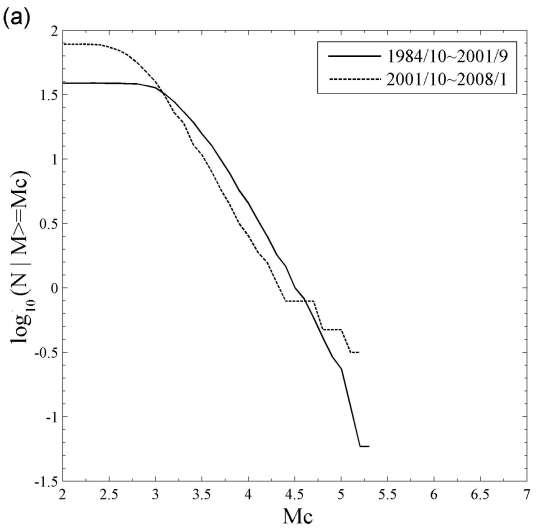

Fig. 1a. The Gutenberg-Richter (GR) frequency-magnitude distribution of two successive intervals, from 1 October 1984 to 30 September 2001, and from 1 October 2001 to 31 January 2008 (UTC), respectively.

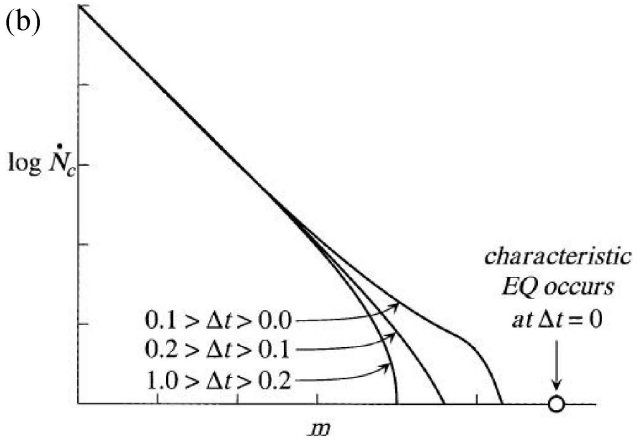

Fig. 1b. The hypothesis of seismic activation for characteristic earthquakes by Rundle et al. (2000). The x-axis is cut-off magnitude, m, and the y-axis is cumulative number of earthquakes which magnitudes are larger than or equal to corresponding m. Δt is a timely ratio measured from the occurrence of a next characteristic earthquake. We have $\Delta t = 1.0$ just after a characteristic earthquake, and the next characteristic earthquake occurs at $\Delta t = 0$. Three Δt stages are indicated from down to up: systematic lack of intermediate-sized earthquakes, a continuous increase of intermediate-sized earthquakes and a further increase of intermediate-sized earthquakes.

which is evaluated by a fitness function. The fitness function is defined by the user for the optimization problem. The fitness measure was used in the process of evolution to determine survival probability of a chromosome. A predefined number of chromosomes composes a population. The size of a population depends on the complexity of the problem in research. An initial population is created in the beginning of GA, and then is used in following iterative evolutions. The values of each gene in the initial population are generated randomly to encompass the solution space as widely as possible.

Evolution of a population in GA consists of three stages: selection, crossover and mutation. After each time evolution, new chromosomes are generated, and elites among them are selected to replace the worst in the original population. A population modified after each time evolution is of a new generation. Evolution is an iterative process until any predefined termination criteria is satisfied: if a known acceptable solution level is attained; or if a maximum number of generations have been performed; or if a given number of generations without fitness improvement. Thus a GA process is completed. The fittest chromosome selected by the fitness measure represents the optimum solution of the problem.

In the selection stage, a chromosome which has a higher fitness measure is a better one. It is given a higher probability to survive and to duplicate offspring in the next generation. The average fitness measure over a population improves after this stage. The crossover procedure is major in the GA process. Two chromosomes are randomly selected from the population as parents. Corresponding parts of each chromosome are selected at identical crossover points and are exchanged to generate offspring. Occurrence of crossover or not depends on a predefined probability. Crossover probabilities up to 80% give satisfying outcomes in many applications (Coley, 1999). An offspring obtains features from both parents.

The mutation procedure provides the opportunity to create new characteristics out of an existing population. Genes of a chromosome are randomly modified subject to a predefined mutation probability. The probability of mutation is about 1∼2% to preserve the stability of the population (Gen and Cheng, 1997). Mutation promotes the diversity of a new generation.

In this research the genes in each chromosome included T_0, T_1, T_2, D_c and M_c, which were important parameters in the PI method. T_3 was defined as 180 days after T_2. Earthquakes which distributed from ground surface to D_c in depth and were larger than M_c in magnitude were used. For each chromosome, the PI method gave a PI map and a RI map by applying the gene set. The number of chromosomes in the initial population was one thousand. The termination condition was to reach the maximum number of generations which was set at one thousand in this research.

The fitness function was the ROC diagram. Performance of each PI map was evaluated by the area confined by the ROC curve and the horizontal and perpendicular axes in the ROC diagram. The PI map which had the largest area in the ROC diagram was evaluated to be the best. Thus the corresponding chromosome was the best result.

4 Results

The best chromosome selected after the GA process was composed of five parameters. Those parameters were T_0: 1 October 1984; T_1: 1 October 2001; T_2: 1 February 2008; D_c: 18 km and M_c: 3.0. Last parameter T_3 was referred to the occurrence time of the Wen-chuan main shock and thus was predefined at 31 July 2008 (UTC). Thus, the baseline interval was from 1 October 1984 to 30 September 2001, and the change interval was from 1 October 2001 to 31 January 2008.

Gutenberg-Richter distributions of both intervals are displayed in Fig. 1a. According to the definition of the Gutenberg-Richter (G-R) law, the x-axis in Fig. 1a was a cut-off magnitude, named Mc in short. For each x-value, only the earthquakes which were equal to or larger than x in magnitude were counted. Then the total number of selected earthquakes during each interval was evaluated as number per year and expressed as a y-value, corresponding to an x-value, on a logarithmic scale. For both intervals, the G-R curves behaved like parallel straight lines from 3.5 to 4.4 in M_c. The slope, which is fitted by linear segment of a G-R curve, was 1.17 for the baseline interval and was 1.23 for the change interval, separately. The slope of the curve, b-value, indicates a relative ratio between smaller earthquakes to larger earthquakes. Similar b-values showed similar composition of earthquakes smaller than 4.4 during both intervals. The straight pattern of the G-R curve for the baseline interval extended to $M_c = 5$. On the other hand, a higher a-value showed that smaller earthquakes were more active during the baseline interval. However, for the change interval, the linearity of the G-R curve broke once M_c exceeded 4.4 and the G-R curve jumped suddenly.

The PI and RI maps obtained by applying the parameter set from the best GA solution are displayed in Fig. 2a and b. In each figure, only one hundred boxes which had the strongest amplitudes were plotted as colored hotspots. The calculation value of each box was divided by the maximum among the selected hotspots and was displayed in a logarithmic scale.

The blue inverted triangles designate the earthquakes during the change interval, from 1 October 2001 to 31 January 2008 (UTC). The green circles show the target earthquakes during the forecasting interval, from 1 February 2008 to 31 July 2008. The threshold of magnitude and depth of the displayed earthquakes were 5.0 and 18 km, respectively. The sizes of the earthquakes were positively proportional to their magnitudes. In simple visual inspection, most of the selected hotspots were located on or close to the epicenters of the Wen-chuan main shock and big aftershocks.

However, a rigorous statistical testing was necessary. The ROC curves for both maps are shown in Fig. 2c. The solid line designates the PI map and dotted line the RI map. The curve for the PI map kept locating above the one for the RI map until the false alarm rate reached 0.6. Furthermore, the

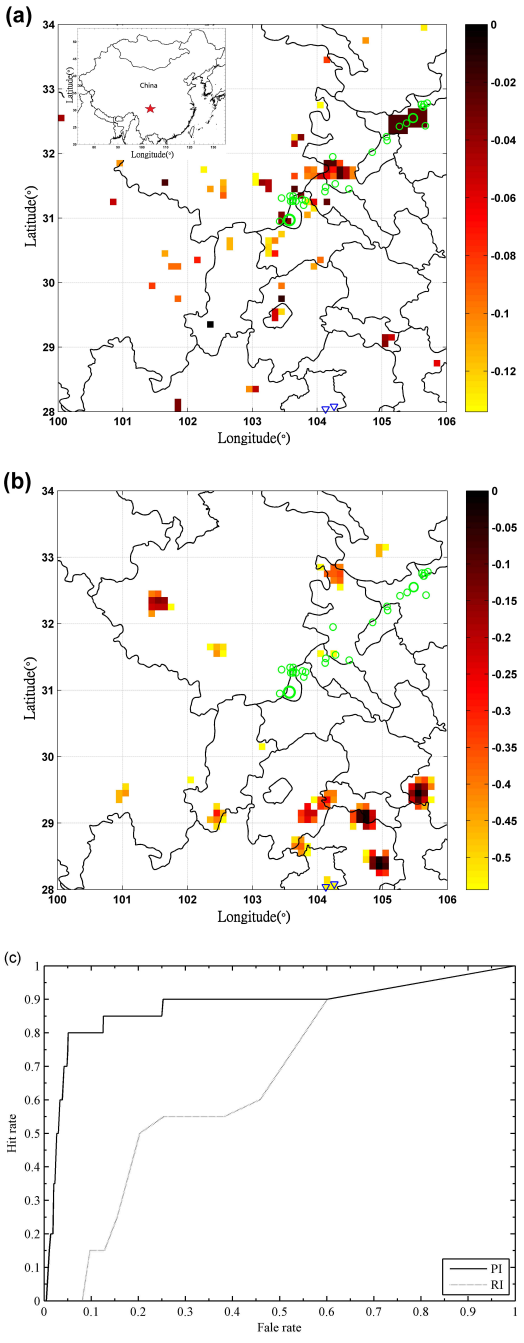

Fig. 2. **(a)** Pattern informatics (PI) map and **(b)** Relative intensity (RI) map. Blue inverted triangles indicate the earthquakes from 1 October 2001 (T_1) to 31 January 2008 and green circles indicate the earthquakes from 1 February 2008 (T_2) to 31 July 2008 (T_3). The magnitude threshold of all displayed earthquakes was 5.0. The values of hotspots were normalized by the respective maximum in each figure and were displayed in logarithmic scales. Red star in the insert indicated the epicenter of the 2008 Wen-chuan, China earthquake. **(c)** Relative operating characteristic (ROC) diagram. ROC diagram evaluated the similarity of spatial distribution between hotspots (in PI or RI map) and the Wen-chuan earthquake sequence. Through comparing areas under curves, the PI map performed better in this testing.

areas under the curves were 0.879 and 0.656, respectively. Through the ROC test, the PI map numerically proved to be a better result.

5 Discussion

In this research, we developed a quick and objective combination method to identify possible seismic anomalies before the 2008 Wen-chuan earthquake. The seismic anomaly displayed in the PI map showed high spatial similarity to the distribution of the Wen-chuan main shock and following big aftershocks. Through studying the characteristics of the identified seismic anomaly, our attempt was to further understand the generation of big earthquakes like the Wen-chuan earthquake.

The sudden jump of the G-R curve for the change interval indicated that, relative to smaller earthquakes, the seismicity larger than 4.4 in magnitude was more active during the interval. We thought that this characteristic represented seismic activation and could be referred to the seismic activation hypothesis proposed by Rundle et al. (2000b).

Rundle's seismic activation hypothesis was developed as a model to explain a recurrence cycle of characteristic earthquakes. The process is illustrated by three G-R law curves in Fig. 1b. For a complete cycle of characteristic earthquake, the interval length between two successive characteristic earthquakes is set to 1. A parameter Δt indicates how time is close to the occurrence of a later characteristic earthquake. The value of Δt is 1 when a previous characteristic earthquake has occurred. While time approaches gradually to a later characteristic earthquake, the value of Δt continuously decreases. The value Δt of reaches 0 when a later characteristic earthquake has occurred. Local seismicity is classified roughly into two types, smaller and intermediate earthquakes, by magnitude. According to the composition of two kinds of earthquakes, a complete cycle of characteristic earthquakes is divided into three stages representing the evolutions of local seismicity. Throughout a cycle, the occurrence rate of smaller earthquakes per unit time keeps nearly constant. This characteristic is displayed by a similar slope of the linear part for each G-R curve. However, the rate of intermediate earthquakes increases while time is approaching to a later characteristic earthquake. In the earlier stage, in which Δt is from 1 to 0.2, there are fewer intermediate earthquakes. This lack is represented by a downward curvature of the corresponding G-R curve. In the middle stage, which Δt is from 0.2 to 0.1, the rate of intermediate earthquakes increases and generates a complete linear G-R curve. In the final stage, the rate of intermediate earthquakes further increases and results in an uplift of the corresponding G-R curve. This characteristic of local seismicity is seismic activation and is taken as an indicator for a later characteristic earthquakes. The values of Δt in all stages only represent how time is close to the occurrence of a later characteristic earthquake. They are not precise separations for each stage in a cycle.

We suggest that the seismicity during the baseline interval behaved like a combination of the first two stages, $1 > \Delta t > 0.1$, and the seismicity during the change interval was in the final stage, $0.1 > \Delta t > 0$, respectively. The evolution of the G-R curves implied that seismic activation was a possible indicator of the Wen-chuan earthquake. But this seismic activation was a mixing result considering the whole region researched. In fact, there were different levels of seismic changes among all boxes. The PI map helped us to further understand the spatial distribution of determined seismic anomaly.

Remembering that spatial distribution of selected hotspots revealed an area which had the strongest seismic anomaly during change interval, the similarity of spatial distribution between selected hotspots and the epicenters of the Wenchuan earthquake sequence in Fig. 2a was really interesting. A similar anomaly pattern around the Wen-chuan mainshock was also reported by Huang using the Region-Time-Length (RTL) method (Huang, 2008). In the RTL method, for a selected location at specific time each earthquake which has occurred near the location and prior to the time is used to evaluate the level of seismicity around it. Influence of each earthquake involved is quantitatively performed by functions for distance from the selected location, occurrence time and rupture length. The RTL parameter is a multiple of the three functions and describes decrease (negative value) or increase (positive value) of seismicity. Although the algorithm of the RTL method is quite different than PI, both methods emphasize correlations of earthquakes in space and time. In Huang's analysis, a seismic quiescence zone is well identified around the epicenter of the 2008 Wen-chuan main shock (as the selected location) by using the CES data from 2006 to 2007. The spatial distribution of the seismic quiescence zone is highly similar to the PI result in Fig. 2a. There seemed to be some kind of spatial-temporal correlation between the strongest seismic anomalies and the future big earthquakes in both results. However, it has still been unable to prove that the seismic anomaly which occurred before the Wen-chuan main shock really affected or induced the occurrence of the Wen-chuan earthquake series.

Another noticeable illustration of seismic activation before big earthquake is the 1999 Chi-chi, Taiwan earthquake (Chen, 2003). The seismic activation is explored in a different way with a variation in correlation coefficient, and is reported to occur during 1994 to 20 September 1999 (UTC). The activation threshold is 5.0 in magnitude, a little bigger than the Wen-chuan event.

The interval of the seismic activation is taken as the change interval, and the baseline interval is taken to begin at 1 November 1987, which is just after the occurrence of another big earthquake. Similar to the result of the Wenchuan earthquake, the PI map evaluated shows high spatial

correlation between selected strongest seismic anomaly and the Chi-chi earthquake series.

Despite the two examples illustrated above, it is still in doubt that seismic activation is a necessary process to generate a big earthquake. Since the combination of GA and PI showed high efficiency in identifying seismic anomaly before big earthquakes, an instant plan is to apply the same strategy to other noticeable big earthquakes around the world, for example, the Haiti and the Chili earthquakes in 2010. We believe that, through collecting more and more information about seismicity before big earthquakes, further understanding the generation process can be expected and is useful in seismic hazard.

Acknowledgements. H. C. Li is grateful for the support of the National Science Council (ROC) and the Institute of Geophysics, NCU (ROC). The work of C. C. Chen is supported by the National Science Council (ROC) and the Department of Earth Sciences, NCU (ROC). The authors thank John Rundle (University of California, Davis, USA) and Kristy F. Tiampo (University of Western Ontario, Canada) for their fundamental work and expert opinions on Pattern Informatics. The authors also thank Luciano Telesca and one anonymous reviewer for their helpful comments. The effort of the China Earthquake Administration to maintain the CDSN is highly appreciated.

Edited by: M. E. Contadakis
Reviewed by: L. Telesca and another anonymous referee

References

Chen, C. C.: Accelerating seismicity of moderate-size earthquakes before the 1999 Chi-Chi, Taiwan, earthquake: Testing time-prediction of the self-organizing spinodal model of earthquakes, Geophys. J. Int., 155, F1–F5, 2003.

Chen, C. C., Rundle, J. B., Holliday, J. R., Nanjo, K. Z., Turcotte, D. L., Li, S. C., and Tiampo, K. F.: The 1999 Chi-chi, Taiwan, earthquake as a typical example of seismic activation and quiescence, Geophys. Res. Lett., 32(22), L22315, doi:10.1029/2005GL023991, 2005.

Chen, C. C., Rundle, J. B., Li, H. C., Holliday, J., Nanjo, K. Z., Turcotte, D. L., and Tiampo, K. F.: From tornadoes to earthquakes: Forecast verification for binary events applied to the 1999 Chi-Chi, Taiwan, earthquake, Terr. Atmos. Ocean. Sci., 17(3), 503–516, 2006.

Coley, D. A.: An Introduction to Genetic Algorithms for Scientists and Engineers, World Scientific Publications, London, UK, 1999.

Densmore, A. L., Ellis, M. A., Li, Y., Zhou, R. J., Hancock, G. S., and Richardson, N.: Active tectonics of the Beichuan and Pengguan faults at the easternmargin of the Tibetan Plateau, Tectonics, 26, TC4005, doi:10.1029/2006TC001987, 2007.

Egolf, D.: Equilibrium regained: From nonequilibrium chaos to statistical mechanics, Science, 287, 101–104, 2000.

Ferguson, C. D., Klein, W., and Rundle, J. B.: Spinodals, scalings, and ergodicity in a threshold model with long-range stress transfer, Phys. Rev. E, 60, 1359–1374, 1999.

Gen, M. and Cheng, R.: Genetic Algorithms and Engineering Design, John Wiley & Sons Inc., New York, USA, 432 pp., 1997.

Goldberg, D. E.: Genetic Algorithms in Search Optimization and Machine Learning, Addison-Wesley Pub. Co. Reading, MA, 432 pp., 1989.

Holland, J. H.: Adaptation in Natural and Artificial Systems: An Introductory Analysis with Applications to Biology, Control, and Artificial Intelligence, University of Michigan Press, Ann Arbor., 228 pp., 1975.

Huang, Q.: Seismicity changes prior to the 8.0 Wenchuan earthquake in Sichuan, China. Geophys. Res. Let., 35, L23308, doi:10.1029/2008GL036270, 2008.

Jolliffe, I. T. and Stephenson, D. B.: Forecast verification: A practitioner's guide in Atmospheric Science, John Wiley, Hoboken, NJ, 240 pp., 2003.

Klein, W., Anghel, M., Ferguson, C. D., Rundle, J. B., and Sá Martins, J. S.: Geocomplexity and the physics of earthquakes, edited by: Rundle, J. B., Turcotte, D. L., and Klein, W., Geophys. Monographs, 120, AGU, Washington, DC, 43–71, 2000.

Long, X. X., Yan, J. P., Sun, H., and Wang, Z. Z.: Study on earthquake tendency in Sichuan-Yunnan Region based on commensurability , J. Catastrophology, 21(3), 81–84, 2006 (in Chinese).

Nanjo, K. Z., Rundle, J. B., Holliday, J., and Turcotte, D. L.: Pattern informatics and its application for optimal forecasting of large earthquakes in Japan, Pure Appl. Geophys., 163, 2417–2432, 2006.

Rundle, J. B., Klein, W., Gross, S., and Turcotte, D. L.: Boltzmann fluctuations in numerical simulations of nonequilibrium lattice threshold systems, Phys. Rev. Lett., 75, 1658–1661, 1995.

Rundle, J. B., Klein, W., Tiampo, K. F., and Gross, S.: Linear pattern dynamics in nonlinear threshold systems, Phys. Rev. E, 61(3), 2418–2431, 2000a.

Rundle, J. B., Klein, W., Turcotte, D. L., and Malamud, B. D.: Precursory seismic activation and critical-point phenomena, Pure Appl. Geophys., 157, 2165–2182, 2000b.

Rundle, J. B., Tiampo, K. F., Klein, W., and Sa' Martins, J. S.: Self-organization in leaky threshold systems: The influence of near-mean field dynamics and its implications for earthquakes, neurobiology, and forecasting, Proc. Nat. Acad. Sci. USA, 99, suppl. 1, 2514–2521, 2002.

Tiampo, K. F., Rundle, J. B., McGinnis, S., Gross, S., and Klein, W.: Mean-field threshold systems and phase dynamics: An application to earthquake fault systems, Europhys. Lett., 60(3), 481–487, 2002.

Tiampo, K. F., Rundle, J. B., and Klein, W.: Premonitory seismicity changes prior to the Parkfield and Coalinga earthquakes in southern California, Tectonophysics, 413, 77–86, 2006.

Tiampo, K. F., Rundle, J. B., Klein, W., Holliday, J., Sá Martins, J. S., and Ferguson, C. D.: Ergodicity in natural earthquake fault networks, Phys. Rev. E., 75, 066107-1, 2007.